

Vibration control for serviceability enhancement of offshore platforms against environmental loadings

Chih-Shiuan Lin^{1,2a}, Feifei Liu^{3b}, Jigang Zhang^{3c},
Jer-Fu Wang^{4d} and Chi-Chang Lin^{*5,6}

¹National Rail Transit Electrification and Automation Engineering Technology Research Center,
The Hong Kong Polytechnic University, Hung Hom, Kowloon, Hong Kong

²Department of Civil Engineering and Engineering Mechanics, Columbia University, New York, NY, USA

³School of Civil Engineering, Qingdao University of Technology, Qingdao, Shandong, China

⁴Department of Civil and Disaster Prevention Engineering, National United University, Miaoli, Taiwan

⁵Department of Construction Engineering, Chaoyang University of Technology, Taichung, Taiwan

⁶Department of Civil Engineering, National Chung Hsing University, Taichung, Taiwan

(Received July 6, 2018, Revised March 22, 2019, Accepted May 10, 2019)

Abstract. Offshore drilling has become a key process for obtaining oil. Offshore platforms have many applications, including oil exploration and production, navigation, ship loading and unloading, and bridge and causeway support. However, vibration problems caused by severe environmental loads, such as ice, wave, wind, and seismic loads, threaten the functionality of platform facilities and the comfort of workers. These concerns may result in piping failures, unsatisfactory equipment reliability, and safety concerns. Therefore, the vibration control of offshore platforms is essential for assuring structural safety, equipment functionality, and human comfort. In this study, an optimal multiple tuned mass damper (MTMD) system was proposed to mitigate the excessive vibration of a three-dimensional offshore platform under ice and earthquake loadings. The MTMD system was designed to control the first few dominant coupled modes. The optimal placement and system parameters of the MTMD are determined based on controlled modal properties. Numerical simulation results show that the proposed MTMD system can effectively reduce the displacement and acceleration responses of the offshore platform, thus improving safety and serviceability. Moreover, this study proposes an optimal design procedure for the MTMD system to determine the optimal location, moving direction, and system parameters of each unit of the tuned mass damper.

Keywords: offshore platform; multiple tuned mass dampers; vibration control; ice load; earthquake engineering

1. Introduction

Offshore platforms are subject to different environmental loads during their service lifetime, such as waves, wind, ice, and earthquakes. In particular, seismic and ice loads must be comprehensively considered because of their severity and unpredictability. Therefore, actions must be taken to ensure that the platform does not fail or collapse during an ice hit or seismic excitation and to prevent damages (Moan 2005). Since the 1960s, offshore platforms have collapsed because of ice loads (Peyton 1966, Bjerkaas 2006, Liu *et al.* 2009). For example, in 1969, a platform in China was destroyed because of repetitive hits by large ice loads with a maximum thickness

of more than 100 cm. In addition, the dynamic behavior of offshore structures under harsh ice and earthquake loadings underwent extensive investigation to protect structural and production facilities, such as an oil drilling platform in Cook Inlet, Alaska, USA (Bjerkaas 2006) and a popular jacket-type platform (i.e., JZ20-2 MUQ) in Bohai Gulf of the East China Sea (Wang *et al.* 2013, Kandasamy *et al.* 2016).

Generally, long-term studies have considered ice to be a dominant loading in high-latitude regions such as the Bohai Gulf. Severe vibrations induced by the continuous crushing of ice jeopardize structural safety and affect the security and comfort of workers (Yang 2000). Furthermore, the degradation of structural resistance induced by the high amplitude of vibrations may result in fatal disasters. Because of differences in geographical location and hydrological effect, different sea areas have different ice load characteristics. In China, Liaodong Bay is a key oil region in the Bohai oil field and is located in unique waters covered with fast ice and floating ice. Fast ice, also referred to as land-fast ice, is sea ice that is fastened to coastlines and the seabed along grounded icebergs. Floating ice is the primary ice feature in the open sea. In addition, ice conditions have intense dynamic features because of waves and currents under large tidal variations. According to field

*Corresponding author, Honorary Distinguished Professor

E-mail: cclin3@nchu.edu.tw

^a Ph. D., Research Associate

E-mail: jason-cs.lin@polyu.edu.hk

^b Ph. D. Candidate

E-mail: feifeiliu2015@163.com

^c Professor

E-mail: jigangzhang@126.com

^d Assistant Professor

E-mail: jfwang@nuu.edu.tw

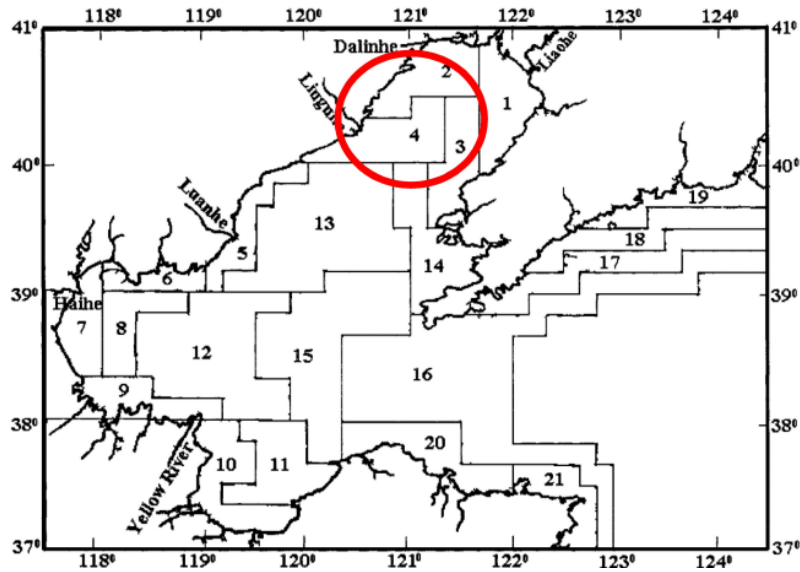


Fig. 1 Ice engineering sub-areas in Bohai Gulf of the East China Sea. (Yang 2000)

observations, sea ice varies with different areas based on the classification of ice engineering subareas in the Bohai Gulf (Li *et al.* 2004). The JZ20-2 MUQ platform examined in this study is located in the fourth area (Fig. 1).

The JZ20-2 MUQ is a four-legged jacket platform comprising a jacket, jacket cap, pillar, helideck, pedestal crane, and breasting dolphin at different elevations (Fig. 2). It has two primary components, namely a substructure and superstructure. The superstructure is supported on a deck, which is fixed on the substructure. Moreover, the superstructure comprises a helideck as well as living and utility modules. The helideck is located at the top of a platform with an elevation of +24.80 m. The living module is at the upper deck at with an elevation of +17.00 m. The utility module is located at the lower deck with an elevation of +13.00 m. The upper deck is primarily used for a living quarter and drilling rig, whereas the lower deck serves as the storage area and system for drilling mud circulation.

In recent decades, the application of passive-type energy dissipation for the vibration control of civil engineering structures against natural and man-induced excitations has received considerable interest from researchers and practicing engineers to ensure structural safety and human comfort (Soong and Dargush 1997, Soong and Spencer 2002, Spencer and Nagarajaiah 2003). Among the devices proposed by the aforementioned researchers, a tuned mass damper (TMD) is one of the most popular devices because of its easy implementation and low interference when incorporated into the existing structures (Lin and Wang 2012). Since the early 1970s, numerous single TMDs have been installed in high-rise buildings and towers, long-span highway bridges, and pedestrian bridges to reduce vibrations because of natural and man-made excitations (Kareem 1983, Xu *et al.* 1992, Lin *et al.* 1999, Debnath and Dutta 2016). Until recently, the parameter design of different TMD systems has remained a dominant research subject (Warnitchai and Hoang 2006, Nigdeli and Bekdas 2013, Nagarajaiah and Jung 2014, Aly 2014, Lucchini *et al.* 2014, Bortoluzzi *et al.* 2015, Salvi and Rizzi 2016,

Ramezani *et al.* 2017). However, relatively few studies have been published on the mitigation of ice-induced vibrations for offshore platforms (Yue *et al.* 2009). Abdel-Rohman (1996) employed a TMD to reduce the vibration caused by self-excited hydrodynamic forces of an offshore steel jacket platform. Alves and Batista (1999) installed a TMD device in the columns of a TLP-type platform to attenuate the amplitude of heave motion. Wang *et al.* (2002) proposed an optimized TMD for a simplified single-degree-of-freedom offshore steel jacket platform. Chandrasekaran *et al.* (2013) placed a TMD at the bottom of a deck plate of a multilegged articulated tower to reduce its bending moment. Recently, the feasibility of the TMD for mitigating the ice-induced vibration of offshore platforms in the Bohai Bay was investigated through experiments (Yue *et al.* 2009, Zhang *et al.* 2017). The results revealed that the TMD can favorably attenuate the ice-induced vibration at offshore platforms.

In a conventional single TMD device, a mass is connected to the primary structure with stiffness and damping elements. In an appropriately designed TMD device, some of the structural energy can be transferred to the TMD and dissipated using the damper (Lin *et al.* 1994, 2001, Wu *et al.* 1999, Wang *et al.* 2009). A single TMD is effective for attenuating the vibration mode of structural systems. To control more than one vibration modes, multiple TMDs (MTMDs) were first introduced by Abe and Igusa in 1995. Moreover, when a single TMD system is not tuned to the desired frequency because of system variations (i.e., the detuning effect), rapid and significant performance degradation is observed. To solve this problem, applying MTMDs for controlling a frequency bandwidth is a favorable solution (Chen and Wu 2003, Lin and Wang 2012).

The proposed MTMD system comprises a parallel arrangement of several TMD units. Each TMD has a mass, natural frequency, and damping ratio. MTMD systems that

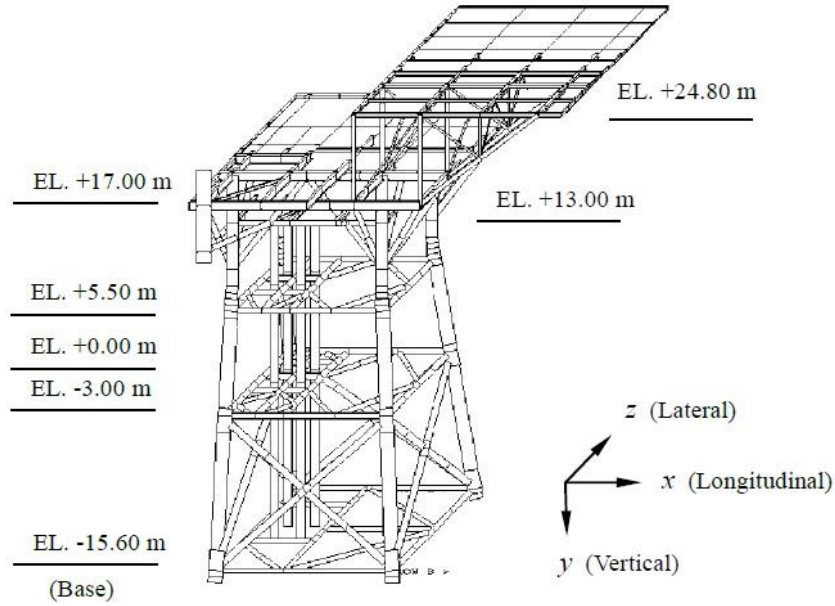


Fig. 2 Configuration of JZ20-2 MUQ platform

create a broader frequency bandwidth than a conventional single TMD can include the variation range of the controlled modal frequency to reduce the detuning effect (Lin *et al.* 2017). Some researchers have investigated the effectiveness of multiple TMDs for suppressing the wave-induced vibration of offshore platforms (Lu *et al.* 2002, Taflanidis *et al.* 2009, Chandrasekaran *et al.* 2013, Zhang *et al.* 2017). They concluded that multiple TMDs outperform a single TMD regarding oscillation amplitude reduction of offshore platforms. In recent years, the authors developed the optimal design methodology for the proposed MTMD system and validated its control performance through extensive analytical studies and large-scale shaking table tests (Lin *et al.* 2010, 2012). In this study, the optimal MTMD system was employed to mitigate the excess vibration of the JZ20-2 offshore platform, which was modeled by the ABAQUS computer program under ice and earthquake loadings. The MTMD system is designed to control the first few dominant coupled modes. The optimal placement and system parameters of the MTMD were determined based on the controlled modal properties. Numerical simulation results revealed that the proposed MTMD system can effectively reduce the displacement and acceleration responses of an offshore platform. Moreover, the optimal design procedure for the MTMD system was proposed to determine the optimal locations, moving directions, and system parameters.

2. Optimal design of MTMD system for platform structures

2.1 Dynamic equations of motion of platform-MTMD systems

The dynamic equations of motion of a general n degrees-of-freedom (DOF) offshore platform structure

equipped with a MTMD system, which consists of p units placed at different locations, under q external ice loadings $\mathbf{F}(t)$ and earthquake excitation in x direction, $\ddot{x}_g(t)$, can be expressed as

$$\mathbf{M}\ddot{\mathbf{x}}(t) + \mathbf{C}\dot{\mathbf{x}}(t) + \mathbf{K}\mathbf{x}(t) = \mathbf{B}\mathbf{F}(t) + \mathbf{M}_f \mathbf{r} \ddot{x}_g(t) \quad (1)$$

in which

$$\mathbf{M} = \begin{bmatrix} \mathbf{M}_p & \mathbf{0} \\ \mathbf{M}_{sp} & \mathbf{M}_s \end{bmatrix}, \quad \mathbf{C} = \begin{bmatrix} \mathbf{C}_p & \mathbf{C}_{ps} \\ \mathbf{0}^T & \mathbf{C}_s \end{bmatrix}, \quad \mathbf{K} = \begin{bmatrix} \mathbf{K}_p & \mathbf{K}_{ps} \\ \mathbf{0}^T & \mathbf{K}_s \end{bmatrix},$$

$$\mathbf{M}_f = \begin{bmatrix} \mathbf{M}_p & \mathbf{0} \\ \mathbf{0}^T & \mathbf{M}_s \end{bmatrix}$$

are $(n+p) \times (n+p)$ mass, damping and stiffness matrices of the entire structure-MTMD system, respectively. \mathbf{M}_p , \mathbf{C}_p , and \mathbf{K}_p are $(n \times n)$ mass, damping and stiffness matrices of the controlled offshore platform structure. The other matrices are expressed in detail as follows

$$\mathbf{M}_s = \begin{bmatrix} m_{s_1} & & & & \\ & \ddots & & & \\ & & m_{s_k} & & \\ & & & \ddots & \\ & & & & m_{s_p} \end{bmatrix}, \quad \mathbf{C}_s = \begin{bmatrix} c_{s_1} & & & & \\ & \ddots & & & \\ & & c_{s_k} & & \\ & & & \ddots & \\ & & & & c_{s_p} \end{bmatrix},$$

$$\mathbf{K}_s = \begin{bmatrix} k_{s_1} & & & & \\ & \ddots & & & \\ & & k_{s_k} & & \\ & & & \ddots & \\ & & & & k_{s_p} \end{bmatrix}$$

are $(p \times p)$ diagonal matrices where m_{s_k} , c_{s_k} , and k_{s_k} are mass, damping and stiffness coefficients of the k th unit of MTMD system ($k=1, 2, \dots, p$); \mathbf{M}_{sp} , \mathbf{C}_{ps} , and \mathbf{K}_{ps}

matrices are expressed, respectively, by

$$\mathbf{M}_{sp} = \mathbf{M}_s \mathbf{v}, \quad \mathbf{C}_{ps} = -(\mathbf{C}_s \mathbf{v})^T, \quad \mathbf{K}_{ps} = -(\mathbf{K}_s \mathbf{v})^T \quad (2a)$$

where

$$\mathbf{v} = \begin{bmatrix} \mathbf{v}_1 \\ \vdots \\ \mathbf{v}_k \\ \vdots \\ \mathbf{v}_p \end{bmatrix}_{(p \times n)} \quad \mathbf{v}_1 = \begin{bmatrix} 0 & \cdots & 1^{(l_1)} & \cdots & 0 \end{bmatrix}_{(1 \times n)} \\ \mathbf{v}_k = \begin{bmatrix} 0 & \cdots & 1^{(l_k)} & \cdots & 0 \end{bmatrix}_{(1 \times n)} \\ \mathbf{v}_p = \begin{bmatrix} 0 & \cdots & 1^{(l_p)} & \cdots & 0 \end{bmatrix}_{(1 \times n)} \quad (2b)$$

In above vector \mathbf{v} , the superscripts $l_1, l_2, \dots, l_k, \dots, l_p$ indicate the DOF indices of the platform structure where the first to the p th TMDs are located. The displacement vector is defined as

$$\mathbf{x}(t) = \begin{Bmatrix} \mathbf{x}_p(t) \\ \mathbf{v}_s(t) \end{Bmatrix} \quad (2c)$$

where $\mathbf{x}_p(t)$ denotes the displacement vector of platform structure relative to the base and $\mathbf{v}_s(t)$ represents the displacement vector of each TMD unit relative to its installed location, called stroke vector. \mathbf{B} is the $(n+p) \times q$ location matrix for the q external ice loadings, $\mathbf{F}(t)$. The $(n+p) \times 1$ influence vector \mathbf{r} has each element equal to -1 . They are expressed as

$$\mathbf{B} = \begin{Bmatrix} \mathbf{b}^{(n \times q)} \\ \mathbf{0}^{(p \times q)} \end{Bmatrix}; \quad \mathbf{r} = \begin{Bmatrix} -\mathbf{1}^{(n \times 1)} \\ -\mathbf{1}^{(p \times 1)} \end{Bmatrix} \quad (2d)$$

Let $\boldsymbol{\eta}(t)$ be the $(n \times 1)$ modal displacement vector and $\boldsymbol{\Phi}$ be the $(n \times n)$ normalized mode shape matrix of the platform structure expressed as

$$\boldsymbol{\Phi} = \begin{bmatrix} \varphi_{(1,1)} & \varphi_{(1,2)} & \cdots & \varphi_{(1,j)} & \cdots & \varphi_{(1,n)} \\ \varphi_{(2,1)} & \varphi_{(2,2)} & \cdots & \varphi_{(2,j)} & \cdots & \varphi_{(2,n)} \\ \vdots & \vdots & \vdots & \vdots & \vdots & \vdots \\ \varphi_{(i,1)} & \varphi_{(i,2)} & \cdots & \varphi_{(i,j)} & \cdots & \varphi_{(i,n)} \\ \vdots & \vdots & \vdots & \vdots & \ddots & \vdots \\ \varphi_{(n,1)} & \varphi_{(n,2)} & \cdots & \varphi_{(n,j)} & \cdots & \varphi_{(n,n)} \end{bmatrix} \quad (2e)$$

where $\varphi_{(i,j)}$ denotes the mode shape value at the i th DOF of the j th mode.

By substituting $\mathbf{x}_p(t) = \boldsymbol{\Phi} \boldsymbol{\eta}(t)$ into Eq. (1) and pre-multiplying two sides of the structure part by $\boldsymbol{\Phi}^T$ to transform the system coordinates from physical domain to modal domain, the modal equations of motion of the combined platform structure-MTMD system become

$$\begin{bmatrix} \mathbf{M}_p^* & \mathbf{0} \\ \mathbf{M}_{sp}^* & \mathbf{M}_s^* \end{bmatrix} \begin{Bmatrix} \ddot{\boldsymbol{\eta}}(t) \\ \ddot{\mathbf{v}}_s(t) \end{Bmatrix} + \begin{bmatrix} \mathbf{C}_p^* & \mathbf{C}_{ps}^* \\ \mathbf{0}^T & \mathbf{C}_s^* \end{bmatrix} \begin{Bmatrix} \dot{\boldsymbol{\eta}}(t) \\ \dot{\mathbf{v}}_s(t) \end{Bmatrix} \\ + \begin{bmatrix} \mathbf{K}_p^* & \mathbf{K}_{ps}^* \\ \mathbf{0}^T & \mathbf{K}_s^* \end{bmatrix} \begin{Bmatrix} \boldsymbol{\eta}(t) \\ \mathbf{v}_s(t) \end{Bmatrix} = \begin{Bmatrix} \mathbf{b}_m \\ \mathbf{0} \end{Bmatrix} \mathbf{F}(t) + \begin{bmatrix} \boldsymbol{\Gamma}_p \\ \boldsymbol{\Gamma}_s \end{bmatrix} \ddot{x}_g(t) \quad (3a)$$

where \mathbf{M}_p^* and \mathbf{M}_s^* are $(n \times n)$ and $(p \times p)$ unity matrices; $\mathbf{C}_p^* = \text{diag}.[2\xi_j \omega_j]$, $\mathbf{K}_p^* = \text{diag}.[\omega_j^2]$ ($j=1, 2, \dots, n$) and $\mathbf{C}_s^* = \text{diag}.[2\xi_{s_k} \omega_{s_k}]$, $\mathbf{K}_s^* = \text{diag}.[\omega_{s_k}^2]$ ($k=1, 2, \dots, p$) are $(n \times n)$ and $(p \times p)$ diagonal matrices, respectively.

$$\mathbf{M}_{sp}^* = \mathbf{v} \boldsymbol{\Phi} = \begin{bmatrix} \varphi_{(1,1)} & \varphi_{(1,2)} & \cdots & \varphi_{(1,j)} & \cdots & \varphi_{(1,n)} \\ \varphi_{(2,1)} & \varphi_{(2,2)} & \cdots & \varphi_{(2,j)} & \cdots & \varphi_{(2,n)} \\ \vdots & \vdots & \vdots & \vdots & \vdots & \vdots \\ \varphi_{(k,1)} & \varphi_{(k,2)} & \cdots & \varphi_{(k,j)} & \cdots & \varphi_{(k,n)} \\ \vdots & \vdots & \vdots & \vdots & \ddots & \vdots \\ \varphi_{(l_p,1)} & \varphi_{(l_p,2)} & \cdots & \varphi_{(l_p,j)} & \cdots & \varphi_{(l_p,n)} \end{bmatrix}_{(p \times n)} \quad (3b)$$

$$\mathbf{C}_{ps}^* = \boldsymbol{\Phi}^T \mathbf{C}_{ps} = \begin{bmatrix} 2\xi_{s_1} \omega_{s_1} \mu_{s_1,1} \varphi_{(1,1)} & 2\xi_{s_2} \omega_{s_2} \mu_{s_2,1} \varphi_{(1,1)} & \cdots & 2\xi_{s_n} \omega_{s_n} \mu_{s_n,1} \varphi_{(1,1)} & \cdots & 2\xi_{s_p} \omega_{s_p} \mu_{s_p,1} \varphi_{(1,1)} \\ 2\xi_{s_1} \omega_{s_1} \mu_{s_1,2} \varphi_{(1,2)} & 2\xi_{s_2} \omega_{s_2} \mu_{s_2,2} \varphi_{(1,2)} & \cdots & 2\xi_{s_n} \omega_{s_n} \mu_{s_n,2} \varphi_{(1,2)} & \cdots & 2\xi_{s_p} \omega_{s_p} \mu_{s_p,2} \varphi_{(1,2)} \\ \vdots & \vdots & \vdots & \vdots & \vdots & \vdots \\ 2\xi_{s_1} \omega_{s_1} \mu_{s_1,j} \varphi_{(1,j)} & 2\xi_{s_2} \omega_{s_2} \mu_{s_2,j} \varphi_{(1,j)} & \cdots & 2\xi_{s_n} \omega_{s_n} \mu_{s_n,j} \varphi_{(1,j)} & \cdots & 2\xi_{s_p} \omega_{s_p} \mu_{s_p,j} \varphi_{(1,j)} \\ \vdots & \vdots & \vdots & \vdots & \ddots & \vdots \\ 2\xi_{s_1} \omega_{s_1} \mu_{s_1,n} \varphi_{(1,n)} & 2\xi_{s_2} \omega_{s_2} \mu_{s_2,n} \varphi_{(1,n)} & \cdots & 2\xi_{s_n} \omega_{s_n} \mu_{s_n,n} \varphi_{(1,n)} & \cdots & 2\xi_{s_p} \omega_{s_p} \mu_{s_p,n} \varphi_{(1,n)} \end{bmatrix}_{(n \times p)} \quad (3c)$$

$$\mathbf{K}_{ps}^* = \boldsymbol{\Phi}^T \mathbf{K}_{ps} = \begin{bmatrix} \omega_{s_1}^2 \mu_{s_1,1} \varphi_{(1,1)} & \omega_{s_2}^2 \mu_{s_2,1} \varphi_{(1,1)} & \cdots & \omega_{s_n}^2 \mu_{s_n,1} \varphi_{(1,1)} & \cdots & \omega_{s_p}^2 \mu_{s_p,1} \varphi_{(1,1)} \\ \omega_{s_1}^2 \mu_{s_1,2} \varphi_{(1,2)} & \omega_{s_2}^2 \mu_{s_2,2} \varphi_{(1,2)} & \cdots & \omega_{s_n}^2 \mu_{s_n,2} \varphi_{(1,2)} & \cdots & \omega_{s_p}^2 \mu_{s_p,2} \varphi_{(1,2)} \\ \vdots & \vdots & \vdots & \vdots & \vdots & \vdots \\ \omega_{s_1}^2 \mu_{s_1,j} \varphi_{(1,j)} & \omega_{s_2}^2 \mu_{s_2,j} \varphi_{(1,j)} & \cdots & \omega_{s_n}^2 \mu_{s_n,j} \varphi_{(1,j)} & \cdots & \omega_{s_p}^2 \mu_{s_p,j} \varphi_{(1,j)} \\ \vdots & \vdots & \vdots & \vdots & \ddots & \vdots \\ \omega_{s_1}^2 \mu_{s_1,n} \varphi_{(1,n)} & \omega_{s_2}^2 \mu_{s_2,n} \varphi_{(1,n)} & \cdots & \omega_{s_n}^2 \mu_{s_n,n} \varphi_{(1,n)} & \cdots & \omega_{s_p}^2 \mu_{s_p,n} \varphi_{(1,n)} \end{bmatrix}_{(n \times p)} \quad (3d)$$

$$\mathbf{b}_m = \boldsymbol{\Phi}^T \mathbf{b}; \quad \boldsymbol{\Gamma}_p = -\boldsymbol{\Phi}^T \mathbf{M}_p \mathbf{1}; \quad \boldsymbol{\Gamma}_s = -\mathbf{1} \quad (3e)$$

where $\varphi_{(i,j)}$ is the mode shape value corresponding to the DOF where the k th TMD is located. $\mu_{s_k,j} = m_{s_k}^* / m_j^*$ is mass ratio of the k th TMD unit to the j th modal effective mass of the structure, m_j^* . ξ_j and ω_j represent the j th modal damping ratio and modal frequency of the platform structure; ξ_{s_k} and ω_{s_k} denote damping ratio and natural frequency of the k th TMD unit, respectively. $\boldsymbol{\Gamma}_p$ indicates the modal participation vector. The dynamic responses of platform structure and MTMD system under ice and/or earthquake loadings can be solved from Eq. (1) or Eq. (3) once the system or modal parameters of the platform structure and MTMD system are obtained by finite element modeling through commercial structural analysis programs or system identification techniques based on real measurements.

2.2 Transfer functions of structure and MTMD under earthquake excitation

In Eq. (3), consider the j th mode of the structure only

and take Fourier transform on both sides. The j th modal displacement of structure and the stroke vector of MTMD can be represented in frequency domain, in terms of transfer functions, as

$$\begin{aligned} \begin{Bmatrix} \eta_j(\omega) \\ \mathbf{v}_s(\omega) \end{Bmatrix} &= \mathbf{A}^{-1} \begin{Bmatrix} \Gamma_{p_j} \\ \Gamma_s \end{Bmatrix} \ddot{X}_g(\omega) \\ &= \begin{bmatrix} H_{pp_j}(\omega) & \mathbf{H}_{ps}(\omega) \\ \mathbf{H}_{sp}(\omega) & \mathbf{H}_{ss}(\omega) \end{bmatrix} \begin{Bmatrix} \Gamma_{p_j} \\ \Gamma_s \end{Bmatrix} \ddot{X}_g(\omega) \end{aligned} \quad (4)$$

In detail

$$\mathbf{A} = \begin{bmatrix} A_j & C_1 & C_2 & \dots & C_k & \dots & C_p \\ D_1 & B_1 & 0 & \dots & 0 & \dots & 0 \\ D_2 & 0 & B_2 & & & & 0 \\ \vdots & \vdots & & \ddots & & & \vdots \\ D_k & 0 & & & B_k & & 0 \\ \vdots & \vdots & & & & \ddots & \vdots \\ D_p & 0 & 0 & \dots & 0 & \dots & B_p \end{bmatrix} \quad (5)$$

where

$$\begin{aligned} A_j &= -\omega^2 + i\omega(2\xi_j\omega_j) + \omega_j^2 \quad ; \\ B_k &= -\omega^2 + i\omega(2\xi_{s_k}\omega_{s_k}) + \omega_{s_k}^2 \\ C_k &= \varphi_{(l,k,j)}\mu_{s_k,j}[-i\omega(2\xi_{s_k}\omega_{s_k}) - \omega_{s_k}^2] \quad ; \quad D_k = \varphi_{(l,k,j)} \\ j &= 1, 2, \dots, n \quad ; \quad k = 1, 2, \dots, p \end{aligned} \quad (6)$$

Then, the j th modal displacement of platform structure and the k th TMD's stroke of the MTMD system can be expressed as

$$\begin{aligned} \eta_j(\omega) &= \left[H_{pp_j}(\omega)\Gamma_{p_j} + \sum_{l=1}^p H_{ps_l}(\omega)\Gamma_{s_l} \right] \ddot{X}_g(\omega) \\ &= H_{\eta_j} \ddot{X}_g(\omega) \\ \mathbf{v}_{s_k}(\omega) &= \left[H_{sp_k}(\omega)\Gamma_{p_j} + \sum_{l=1}^p H_{ss(k,l)}(\omega)\Gamma_{s_l} \right] \ddot{X}_g(\omega) \\ &= H_{v_{s_k}} \ddot{X}_g(\omega) \end{aligned} \quad (7)$$

where $v_{s_k}(\omega)$ represents the k th element of $\mathbf{v}_s(\omega)$. Γ_{s_l} represents the l th element of Γ_s . $H_{ps_l}(\omega)$ and $H_{sp_l}(\omega)$ indicate the l th elements of $\mathbf{H}_{ps}(\omega)$ and $\mathbf{H}_{sp}(\omega)$, respectively. $H_{ss(k,l)}(\omega)$ represents the element at the k th row and l th column of $\mathbf{H}_{ss}(\omega)$. It is noticeable that $\eta_j(\omega)$ represents the modified j th modal displacement of the platform structure with the existence of MTMD system. The reduction of $\eta_j(\omega)$ indicates the control effectiveness of the MTMD system.

2.3 Performance index and optimal parameters of MTMD system

From Eqs. (7) and (8), it has been found that to reduce

the j th modal response, the k th TMD is best located at the DOF where the j th mode shape value is the largest and moves in the direction which the j th mode participates the most. In addition, from Eq. (7), the MTMD's control effectiveness can be evaluated by the performance index, R_j , defined as

$$R_j = \frac{E[\eta_j^2(\omega)]_{\text{with MTMD}}}{E[\eta_j^2(\omega)]_{\text{w/o MTMD}}} \quad (9)$$

representing the j th modal mean square displacement response ratio of the platform structure with and without MTMD. R_j is a function of the j th modal damping ratio, ξ_j , the j th mode shape value corresponding to each TMD's location, $\varphi_{(l,k,j)}$, the mass ratio of the k th MTMD unit mass to the j th modal effective mass of the structure, $\mu_{s_k,j}$, damping ratio of the k th MTMD unit, ξ_{s_k} , and frequency ratio of the k th MTMD unit to the j th modal frequency of the structure, $r_{f_k} (= \omega_{s_k} / \omega_j)$, where $k=1, 2, \dots, p$. With the known structural modal parameters, ω_j , ξ_j , and $\varphi_{(l,k,j)}$ extracted from structural analysis program and the consideration of low cost and easy construction, identical stiffness coefficient, k_{s_0} , and damping coefficient, c_{s_0} , for each MTMD unit are proposed. They have been derived and expressed as

$$k_{s_0} = \frac{m_{st}}{\sum_{k=1}^p \frac{1}{\omega_j^2 r_{f_k}^2}} \quad ; \quad c_{s_0} = \frac{2\xi_{s_0}}{\omega_j} k_{s_0} \quad ; \quad m_{s_k} = \frac{k_{s_0}}{r_{f_k}^2 \omega_j^2} \quad (10)$$

where m_{st} is the total mass of all MTMD units and ξ_{s_0} is a constant (Lin *et al.* 2010, Lin and Wang 2012). Moreover, with an assigned MTMD mass ratio, $\mu_{st,j} = (\sum_{k=1}^p \varphi_{(l,k,j)} m_{s_k}) / m_j^*$, the modal mass ratio of the k th MTMD unit can be calculated by

$$\mu_{s_k,j} = \mu_{st,j} \frac{1/r_{f_k}^2}{\sum_{l=1}^p 1/r_{f_l}^2} \quad (11)$$

With free frequency distribution of MTMD units, the optimization of MTMD system with identical stiffness and damping coefficients involves $(p+1)$ independent parameters, i.e., $r_{f_1}, r_{f_2}, \dots, r_{f_p}$ and ξ_{s_0} . Theoretically, with given $\mu_{st,j}$, ω_j , ξ_j and $\varphi_{(l,k,j)}$, the optimal MTMD's parameters, $(r_{f_1})_{\text{opt}}, (r_{f_2})_{\text{opt}}, \dots, (r_{f_p})_{\text{opt}}$, and $(\xi_{s_0})_{\text{opt}}$, can be obtained by solving the following system of equations generated by differentiating R_j with respect to the $(p+1)$ parameters and equating to zero, respectively, to minimize R_j .

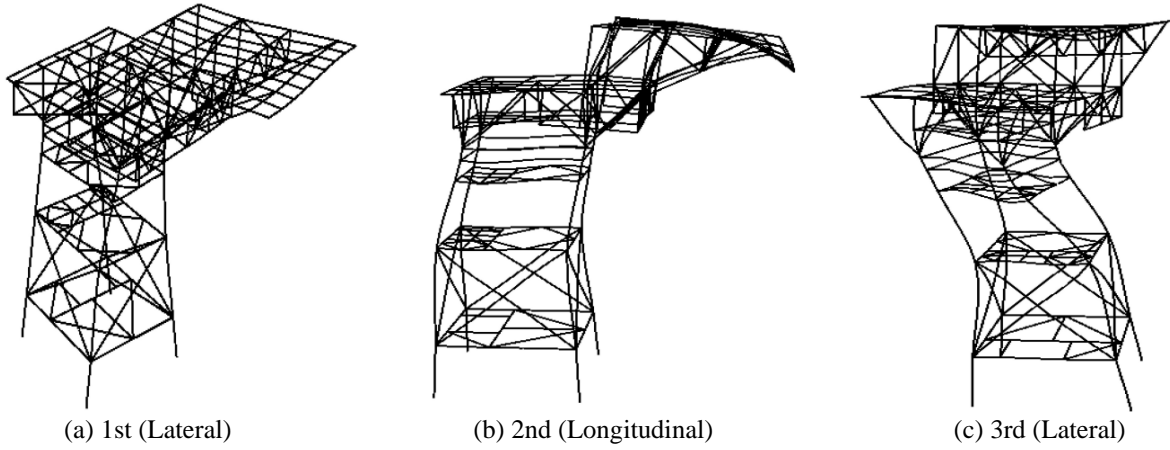


Fig. 3 The first three mode shapes of the JZ20-2 MUQ platform

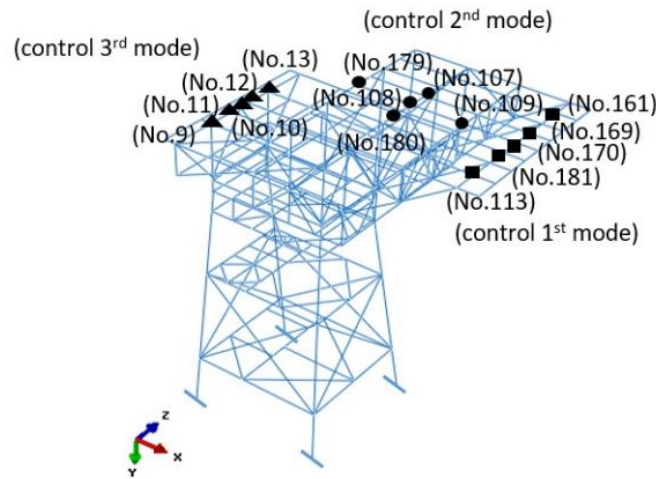


Fig. 4 Locations of MTMD system to control the 1st, 2nd and 3rd modes

Table 1 Modal frequencies, modal masses and modal damping ratios of the first five modes

Controlled mode	Modal frequency (Hz)	Modal mass (ton)	Modal damping ratio (%)
1 st Mode (Lateral)	0.89	171.986 (16%)	3.743
2 nd Mode (Longitudinal)	1.08	769.915 (70%)	3.469
3 rd Mode (Lateral)	1.49	662.239 (64%)	3.303
4 th Mode (Longitudinal)	1.66	75.133 (6.8%)	3.322
5 th Mode (Lateral)	2.14	5.16 (0.5%)	3.352

$$\frac{\partial R_j}{\partial r_{f_1}} = 0, \quad \frac{\partial R_j}{\partial r_{f_2}} = 0, \quad \dots, \quad \frac{\partial R_j}{\partial r_{f_p}} = 0, \quad \frac{\partial R_j}{\partial \xi_{s_0}} = 0 \quad (12)$$

Then, the optimal stiffness coefficient, $(k_{s_0})_{opt}$, damping coefficient, $(c_{s_0})_{opt}$, and mass for the k th MTMD unit, $(m_{s_k})_{opt}$, can be obtained from Eq. (10). The optimization process can be performed by many numerical searching

techniques, which are available in mathematical software packages, such as MATLAB.

3. Optimal MTMD system for the JZ20-2 MUQ platform

The JZ20-2 MUQ platform shown in Fig. 2 was considered as the target structure to design its optimal MTMD system to

reduce excessive vibrations at the helideck and upper deck due to extreme ice loads and through the piles. It is mainly made of steel with density of 7.85 kg/m^3 , Young's modulus of $2.06 \times 10^5 \text{ MPa}$, and Poisson's ratio of 0.3. According to design drawings and details, the commercial finite element program ABAQUS (V14) was employed to model the structure and calculate its modal parameters. The steel beams are modeled with element B31. The mass is simulated as isotropic mass and the total mass of the platform is 1131.257 metric ton (t). Table 1 shows the first five modal frequencies, effective masses, and damping ratios, which were observed from the field. It is seen that the first three modes dominate the lateral (z direction) and longitudinal (x direction) responses with accumulated effective modal mass ratio up to 80% and 70%, respectively. Their corresponding mode shapes are illustrated in Fig. 3. Therefore, a MTMD system is designed to control the first three modes with 5 units ($p = 5$) for each mode. Their optimum locations are shown in Fig. 4.

3.1 Optimal MTMD system parameters

According to the design procedure mentioned in section 2.3, the optimal system parameters of three groups of MTMD system to control the 1st, 2nd, and 3rd modes are determined.

Table 2 MTMD parameters for controlling 1st to 3rd modes

1 st mode					
TMD No.	Node	Mass (ton)	Stiffness (kN/m)	Frequency (Hz)	Damping (kN-s/m)
1	161	0.44		0.93	
2	169	0.50		0.87	
3	170	0.40	14.95	0.97	0.17
4	181	0.35		1.04	
5	113	0.57		0.82	
2 nd mode					
TMD No.	Node	Mass (ton)	Stiffness (kN/m)	Frequency (Hz)	Damping (kN-s/m)
1	109	1.70		1.29	
2	107	1.94		1.21	
3	108	2.21	111.88	1.13	1.18
4	180	2.94		0.98	
5	179	2.52		1.06	
3 rd mode					
TMD No.	Node	Mass (ton)	Stiffness (kN/m)	Frequency (Hz)	Damping (kN-s/m)
1	13	2.20		1.38	
2	12	1.79		1.53	
3	11	1.47	166.47	1.69	0.89
4	10	1.97		1.46	
5	9	1.62		1.61	

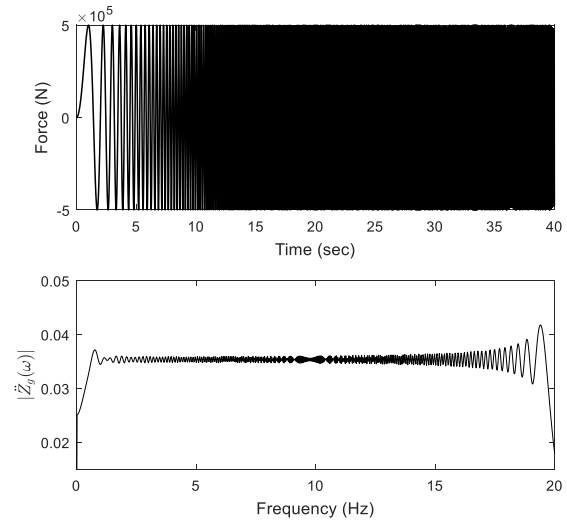


Fig. 5 Swept-sine signal (above) and corresponding Fourier amplitude spectrum (below)

Considering the available space and local member capacity, a total mass ratio of 1% to the platform mass is used to control two horizontal (lateral and longitudinal) responses, respectively, to increase the controlled modal damping ratios above 5%. The mass is distributed to each mode based on the modal effective mass ratio in each direction. Hence, the mass ratios to control the 1st, 2nd, and 3rd mode are $\mu_1 = 0.2\%$, $\mu_2 = 1\%$, and $\mu_3 = 0.8\%$, respectively. Table 2 lists the system parameters of the three MTMD groups. Each MTMD's unit has different mass, but identical stiffness coefficient and damping coefficient to reduce construction error and cost.

To have same mean-square modal acceleration response, it can be found that the equivalent damping ratios of the first three modes are increased to 6.53%, 6.73%, and 5.6%, respectively, through the application of the MTMD systems (Lin *et al.* 2001).

4. Control performance of MTMD system

A swept-sine signal with frequency bandwidth of 0.1-20 Hz, magnitude of $5 \times 10^5 \text{ kN}$, sampling time of 0.02 second, and total duration of 40 seconds is used to simulate the ice loading and base excitation to examine the dynamic behavior of the JZ20-2 platform with and without MTMD systems. Its time history and Fourier amplitude spectrum are shown in Fig. 5. The control performance of the proposed MTMD system is evaluated through the reduction of acceleration responses at helideck and upper deck of the platform under two types of ice loadings and earthquake excitation.

4.1 Dynamic responses due to ice loadings

Bohai Gulf is one of the sea areas with serious ice condition in China. Since last century, ice condition to a large scale has happened seven times in this area. In this study, an actual ice, called bending ice, load with return

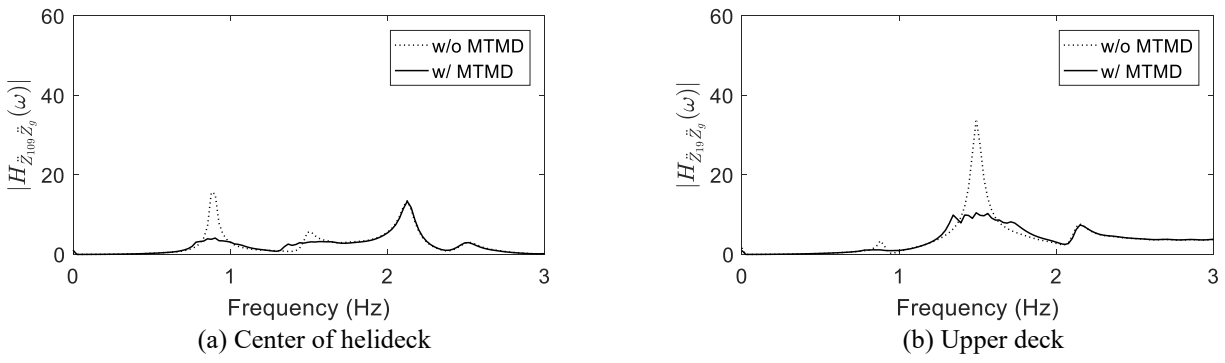


Fig. 6 Acceleration transfer functions due to ice loading applied at four legs in lateral (z) direction

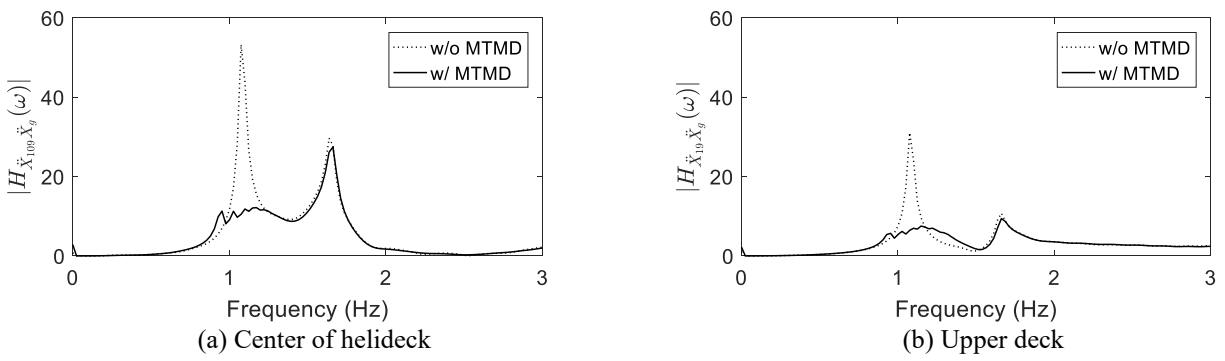


Fig. 7 Acceleration transfer functions due to ice loading applied at four legs in longitudinal (x) direction

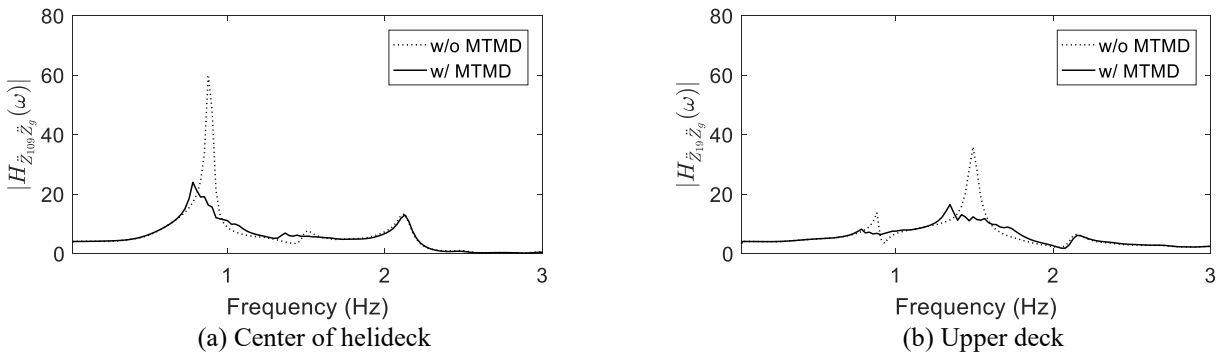


Fig. 8 Acceleration transfer functions due to base acceleration in lateral (z) direction

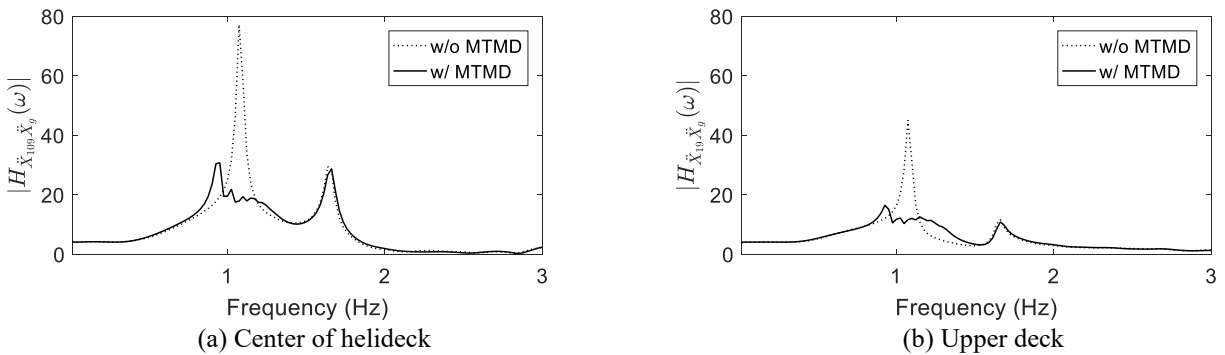


Fig. 9 Acceleration transfer functions due to base acceleration in longitudinal (x) direction

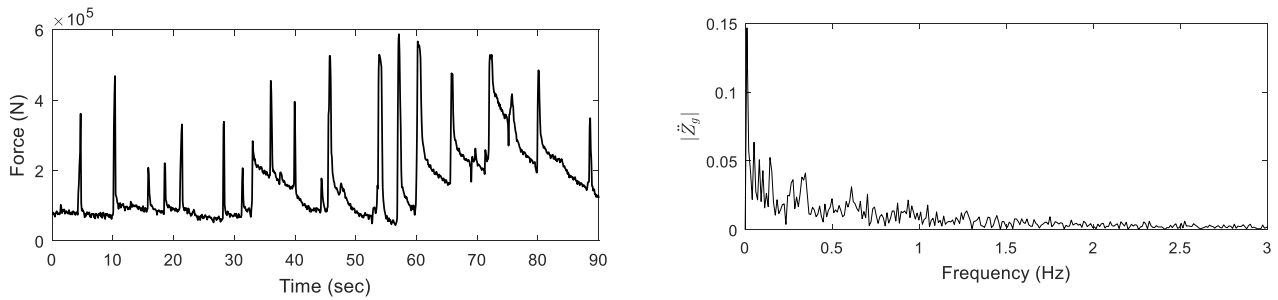


Fig. 10 Time history (above) and Fourier amplitude spectrum (below) of bending ice load

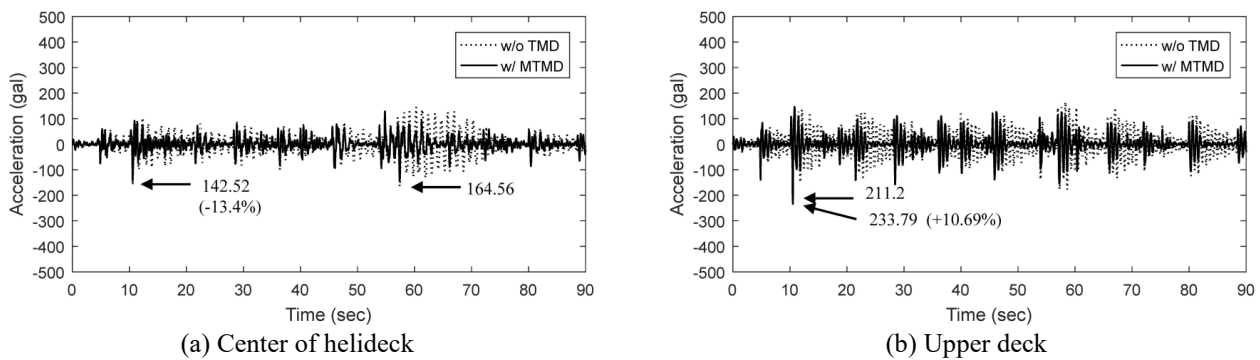


Fig. 11 Acceleration responses due to bending ice loading in lateral direction

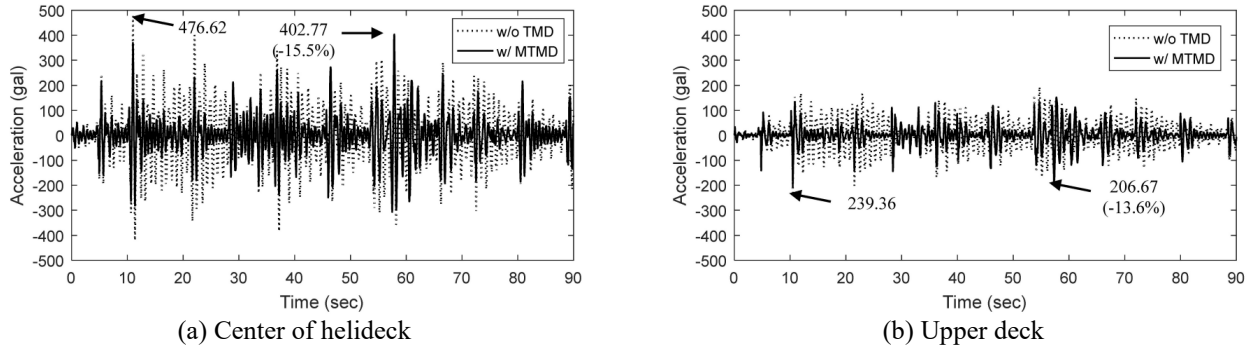


Fig. 12 Acceleration responses due to bending ice loading in longitudinal direction

period of 50 years is assumed to excite at four legs at EL. 4 m above sea level along both lateral and longitudinal directions. For the JZ20-2 platform, it is observed from Fig. 3 that the helideck and upper deck show higher modal deformation in two horizontal directions. In addition, crew members may be evoked discomfort due to excessive acceleration vibration at two decks during ice or seismic excitations. In view of this, the mitigation of vibration responses at center of both decks is very important and considered for the demonstration of control performance of MTMD system.

The time history of actual bending ice loading and its corresponding Fourier amplitude spectrum are shown in Fig. 10. The time history of loading was measured from a real offshore platform located at Bohai Gulf. The Fourier amplitude spectrum of the loading ice force was calculated

by using the MATLAB function `fft()`. It is seen that its dominant frequency contents are below 2.0 Hz. The acceleration responses at the center of two decks of the platform with and without the proposed MTMD systems are illustrated in Figs. 11 and 12. It is seen that two horizontal responses are obviously reduced. The root-mean-square (RMS) responses are reduced near 40% by using the MTMD system with mass ratio of only 1% in each horizontal direction as shown in Table 3.

Vibration problem may influence the crew members both physiologically and psychologically when working and living in a vibration environment for long period of time, and even threaten their health. The effects of vibration are largely related to four factors, i.e., acceleration amplitude, frequency, duration, and direction. The serviceability of a platform in terms of crew discomfort can be assessed by

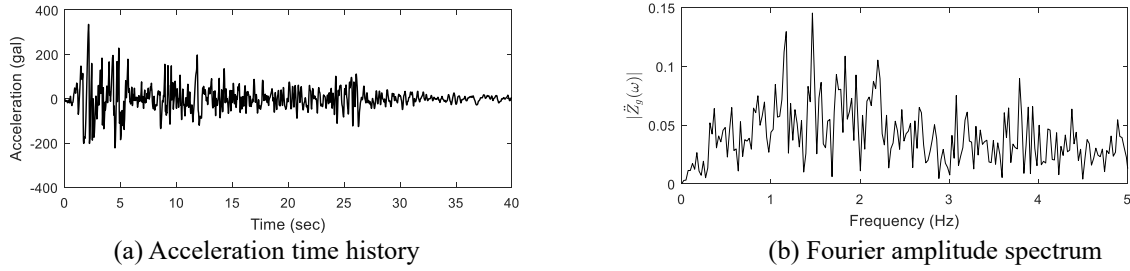


Fig. 13 1940 El Centro earthquake

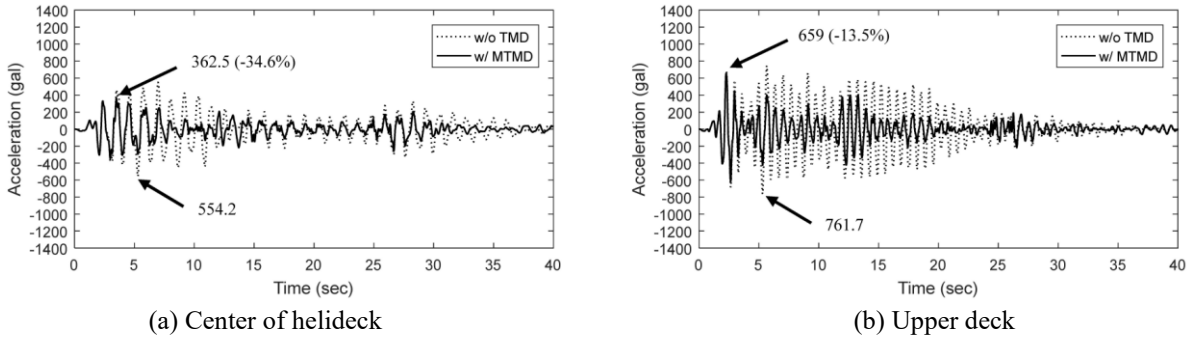


Fig. 14 Acceleration responses due to earthquake excitation in lateral direction

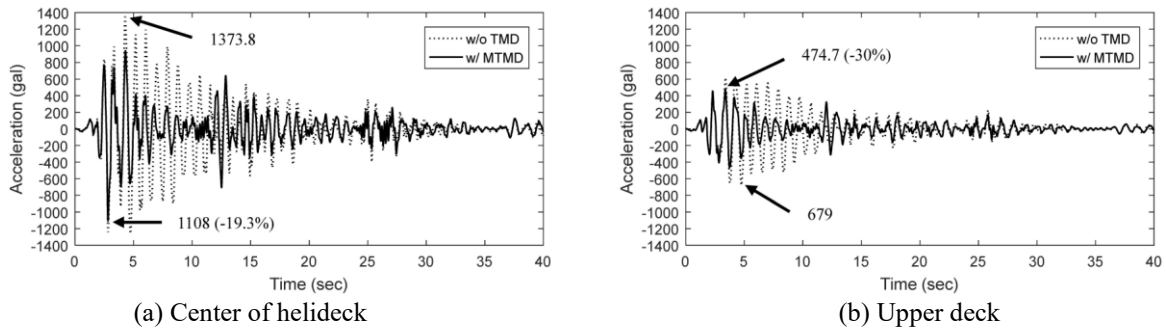


Fig. 15 Acceleration responses due to earthquake excitation in longitudinal direction

using standards on human exposure to vibrations. In this study, three evaluations are made on Bohai Sea platforms, such as comfort degradation, decline of working efficiency and exposure time. The Chinese standard “Reduced Comfort Boundary and Evaluation Criteria for Human Exposure to Whole-body Vibration” (GB/T 13442-1992, 1992) is used for the evaluation. In China, the evaluation standard was established with reference to ISO 2631-1 and revised by its own experiments (ISO 2631, 1997). Table 4 shows the bounds of the RMS acceleration as a function of the time of exposure in GB/T 13442-92. These bounds are given for vibration frequencies less than 2 Hz. Level I is comfort degradation limit, II is work efficiency degradation limit, and III is exposure limitation. II is 3.15 times as great as I, and III is 2.0 times greater than II. Therefore, according to the standard of GB/T 13442-92, it is found that the proposed MTMD system is effective in increasing the work efficiency and exposure time based on the vibration reduction at upper deck, and sufficient time for evacuation based on that at helideck.

4.2 Dynamic responses due to earthquake excitation

As investigated in last section, the 1940 El Centro earthquake is assumed to excite at the base (EL. -15.6 m) of the platform along both lateral and longitudinal directions. Its time history and Fourier amplitude spectrum are shown in Fig. 13. It is found that the first five modes of the platform are located within the dominant frequency range (0.5 to 3.0 Hz) of the earthquake. Figs. 14 and 15 show the time history of acceleration responses at the center of helideck and upper deck for the platform without and with the proposed MTMD system under earthquake excitation in lateral and longitudinal directions. It is seen that the horizontal responses at two decks are significantly reduced. Table 5 shows the RMS responses are reduced up to 50% indicating the control effectiveness of the proposed MTMD system.

Table 3 Control performance of MTMD under bending ice loading

Direction	Location	RMS Acceleration (gal)		Reduction (%)
		Uncontrolled	Controlled	
Lat. (z)	Helideck	42.57	25.83	39.34
	Upper deck	52.6	35.55	32.41
Long. (x)	Helideck	116.87	74.97	35.85
	Upper deck	61.44	37.11	39.60

Table 4 Critical value of human tolerance on vibration acceleration and duration (Unit: gal)

	1 min	16 min	25 min	1 hr	2.5 hr	4 hr	8 hr	16 hr	24 hr
I	63.0	48.0	40.0	27.0	16.0	11.0	7.0	5.0	3.0
II	198.5	151.2	126.0	85.1	50.4	34.7	22.1	15.8	9.5
III	397	302.4	252.0	170.2	100.8	69.4	44.2	31.6	19.0

Table 5 Control performance of MTMD system under earthquake excitation

Direction	Location	RMS Acceleration (gal)		Reduction (%)
		Uncontrolled	Controlled	
Lat. (z)	Helideck	168.5	93.6	44.5
	Upper deck	251.5	125	50.3
Long. (x)	Helideck	329	193.2	41.3
	Upper deck	176.5	102.5	41.9

5. Conclusions

In this study, an optimal MTMD system is proposed to mitigate excessive acceleration responses of the JZ20-2 offshore platform located at Bohai Gulf of the East China Sea. Both extreme ice force and earthquake acceleration are assumed to excite at the structure and the base, respectively. The RMS accelerations at helideck and upper deck of the platform are investigated to examine the comfort condition, work efficiency, and exposure time of workers. Three groups of MTMD system with five units each are designed to control the first three modes of the platform structure. A total of 1% mass ratio is used for each control direction to increase all controlled modal damping ratio above 5%. Their optimum locations, moving direction and system parameters are determined based on the minimization of modal displacement response with and without MTMD system. The commercial finite element program ABAQUS was employed to model the offshore platform structure and calculate its modal parameters and dynamic responses under different environmental loadings. Numerical simulation results showed that the proposed MTMD system is able to reduce acceleration responses significantly at two decks of the JZ20-2 platform to enhance its equipment

functionality and human comfort, work efficiency, and safety.

References

- Abdel-Rohman, M. (1996), "Structural control of a steel jacket platform", *Struct. Eng. Mech.*, **4**(2), 125-138. <https://doi.org/10.12989/sem.1996.4.2.125>.
- Abe, M. and Igusa, T. (1995), "Tuned mass dampers for structures with closely spaced natural frequencies", *Earthq. Eng. Struct. D.*, **24**(2), 247-261. <https://doi.org/10.1002/eqe.4290240209>.
- Alves, R.M. and Batista, R.C. (1999), "Active/passive control of heave motion for TLP type of offshore platforms", *Proceedings of the 9th International Offshore and Polar Engineering Conference (ISOPE)*, Brest, France.
- Aly, A.M. (2014), "Vibration control of high-rise buildings for wind: a robust passive and active tuned mass damper", *Smart Struct. Syst.*, **13**(3), 473-500. <https://doi.org/10.12989/sss.2014.13.3.473>.
- Bjerkås, M. (2006), "Wavelet transforms and ice actions on structures", *Cold Reg. Sci. Technol.*, **44**(2), 159-169. <https://doi.org/10.1016/j.coldregions.2005.11.003>.
- Bortoluzzi, D., Casciati, S., Elia, L. and Faravelli, L. (2015), "Design of a TMD solution to mitigate wind-induced local vibrations in an existing timber footbridge", *Smart Struct. Syst.*, **16**(3), 459-478. <http://dx.doi.org/10.12989/sss.2015.16.3.459>.
- Chandrasekaran, S., Kumar, D. and Ramanathan, R. (2013), "Dynamic response of tension leg platform with tuned mass dampers", *J. Naval Archit. Mar. Eng.*, **10**(2), 1813-8235. <https://doi.org/10.3329/jname.v10i2.16184>.
- Chen, G. and Wu, J. (2003), "Experimental study on multiple tuned mass dampers to reduce seismic responses of a three-story building structure", *Earthq. Eng. Struct. D.*, **32**(5), 793-810. <https://doi.org/10.1002/eqe.249>.
- Debnath, N. and Dutta, A. (2016), "Multi-modal vibration control of truss bridges with tuned mass dampers under general loading", *J. Vib. Control*, **22**(20), 4121-4140. <https://doi.org/10.1177/1077546315571172>.
- GB/T 13442-1992 (1992), *Reduced Comfort Boundary and Evaluation Criteria for Human Exposure to Whole-Body Vibration*, Standardization Administration of China; Beijing, China.
- ISO 2631-1 (1997), *Evaluation of Human Exposure to Whole-Body Vibration. Part1: General requirements*, International Standard Organization for Standardization; Geneva, Switzerland.
- Kareem, A. (1983), "Mitigation of wind induced motion of tall buildings", *J. Wind Eng. Ind. Aerod.*, **11**(1-3), 273-284. [https://doi.org/10.1016/0167-6105\(83\)90106-X](https://doi.org/10.1016/0167-6105(83)90106-X).
- Kandasamy, R., Cui, F., Townsend, N., Foo, C.C., Guo, J., Sheno, A. and Xiong, Y. (2016), "A review of vibration control methods for marine offshore structures", *Ocean Eng.*, **127**, 279-297. <https://doi.org/10.1016/j.oceaneng.2016.10.001>.
- Li, Z., Lu, P. and Sodhi, D. (2004), "Ice engineering sub-areas in Bohai from ice physical and mechanical parameters", *Adv. Water Sci.*, **15**(5), 598-602. [in Chinese]
- Lin, C.C., Hu, C.M., Wang, J.F. and Hu, R.Y. (1994), "Vibration control effectiveness of passive tuned mass dampers", *J. Chin. Inst. Eng.*, **17**(3), 367-376. <https://doi.org/10.1080/02533839.1994.9677600>.
- Lin, C.C., Ueng, J.M. and Huang, T.C. (2000), "Seismic response reduction of irregular buildings using passive tuned mass dampers", *Eng. Struct.*, **22**(5), 513-524. [https://doi.org/10.1016/S0141-0296\(98\)00054-6](https://doi.org/10.1016/S0141-0296(98)00054-6).
- Lin, C.C., Wang, J.F. and Ueng, J.M. (2001), "Vibration control identification of seismically-excited MDOF structure-PTMD

- systems”, *J. Sound Vib.*, **240**(1), 87-115. <https://doi.org/10.1006/jsvi.2000.3188>.
- Lin, C.C., Wang, J.F., Lien, C.H., Chiang, H.W. and Lin, C.S. (2010), “Optimum design and experimental study of multiple tuned mass dampers with limited stroke”, *Earthq. Eng. Struct. D.*, **39**(14), 1631-1651. <https://doi.org/10.1002/eqe.1008>.
- Lin, C.C. and Wang, J.F. (2012), Optimal Design and Practical Considerations of Tuned Mass Dampers for Structural Control, Chapter 6 of the book on *Design Optimization of Active and Passive Structural Control Systems*, (Eds., Nikos D. Lagaros, V. Plevris, and Chara C. Mitropoulou), IGI Global Publisher, USA.
- Lin, C.C., Lin, G.L. and Chiu, K.C. (2017), “Robust design strategy for multiple tuned mass dampers with consideration of frequency bandwidth”, *Int. J. Str. Stab. Dyn.*, **17**(1), 1750002. <https://doi.org/10.1142/S021945541750002X>.
- Liu, X., Li, G., Yue, Q. and Oberlies, R. (2009), “Acceleration-oriented design optimization of ice-resistant jacket platforms in the Bohai Gulf”, *Ocean Eng.*, **36**(17-18), 1295-1302. <https://doi.org/10.1016/j.oceaneng.2009.09.008>.
- Lu, J., Mei, N., Li, Y. and Shi, X. (2002), “Vibration control of multi tuned mass dampers for an offshore oil platform”, *China Ocean Eng.*, **16**(3), 321-328.
- Lucchini, A., Greco, R., Marano, G.C. and Monti, G. (2014), “Robust design of tuned mass damper systems for seismic protection of multistory buildings”, *J. Struct. Eng. - ASCE*, **140**(8), A4014009. [https://doi.org/10.1061/\(ASCE\)ST.1943-541X.0000918](https://doi.org/10.1061/(ASCE)ST.1943-541X.0000918).
- Moan, T. (2005), “Safety of offshore structures”, CORE Report No. 2005-04; Centre for Offshore Research and Engineering, National University of Singapore, Singapore.
- Nagarajaiah, S. and Jung, H.J. (2014), “Smart tuned mass dampers: recent developments”, *Smart Struct. Syst.*, **13**(2), 173-176. <https://doi.org/10.12989/sss.2014.13.2.173>.
- Nigdeli, S.M. and Bekdas, G. (2013), “Optimum tuned mass damper design for preventing brittle fracture of RC buildings”, *Smart Struct. Syst.*, **12**(2), 137-155. <https://doi.org/10.12989/sss.2013.12.2.137>.
- Peyton, H.R. (1966), “Sea Ice Strength”, Report No. UAG R-182, Geophysical Institute, University of Alaska, Alaska.
- Ramezani, M., Bathaei, A. and Zahrai, S.M. (2017), “Designing fuzzy systems for optimal parameters of TMDs to reduce seismic response of tall buildings”, *Smart Struct. Syst.*, **19**(3), 269-277. <https://doi.org/10.12989/sss.2017.19.3.269>.
- Salvi, J. and Rizzi, E. (2016), “Closed-form optimum tuning formulas for passive Tuned Mass Dampers under benchmark excitations”, *Smart Struct. Syst.*, **17**(2), 231-256. <https://doi.org/10.12989/sss.2016.17.2.231>.
- Soong, T.T. and Dargush, G.F. (1997), *Passive Energy Dissipation Systems in Structural Engineering*, Wiley, Buffalo.
- Soong, T.T. and Spencer Jr, B.F. (2002), “Supplemental energy dissipation: state-of-the-art and state-of-the practice”, *Eng. Struct.*, **24**(3), 243-259. [https://doi.org/10.1016/S0141-0296\(01\)00092-X](https://doi.org/10.1016/S0141-0296(01)00092-X).
- Spencer Jr, B.F. and Nagarajaiah, S. (2003), “State of the art of structural control”, *J. Struct. Eng. - ASCE*, **129**(7), 845-856. [https://doi.org/10.1061/\(ASCE\)0733-9445\(2003\)129:7\(845\)](https://doi.org/10.1061/(ASCE)0733-9445(2003)129:7(845)).
- Taflanidis, A.A., Angelides, D.C. and Scruggs, J.T. (2009), “Simulation-based robust design of mass dampers for response mitigation of tension leg platforms”, *Eng. Struct.*, **31**(4), 847-857. <https://doi.org/10.1016/j.engstruct.2008.11.014>.
- Wang, S., Li, H., Ji, C. and Jiao, G. (2002), “Energy analysis for TMD structure systems subjected to impact loading”, *China Ocean Eng.*, **16**(3), 301-310.
- Wang, J.F., Lin, C.C. and Lien, C.H. (2009), “Two-Stage optimum design of tuned mass dampers with consideration of stroke”, *Struct. Control Health Monit.*, **16**(1), 55-72. <https://doi.org/10.1002/stc.312>.
- Wang, S., Yue, Q. and Zhang, D. (2013), “Ice-induced non-structure vibration reduction of jacket platforms with isolation cone system”, *Ocean Eng.*, **70**, 118-123. <https://doi.org/10.1016/j.oceaneng.2013.05.018>.
- Warnitchai, P. and Hoang, N. (2006), “Optimal placement and tuning of multiple tuned mass dampers for suppressing multi-mode structural response”, *Smart Struct. Syst.*, **2**(1), 1-24. <https://doi.org/10.12989/sss.2006.2.1.001>.
- Wu, J., Chen, G. and Lou, M. (1999), “Seismic effectiveness of tuned mass dampers considering soil-structure interaction”, *Earthq. Eng. Struct. D.*, **28**(11), 1219-1233.
- Xu, Y.L., Kwok, K.C.S. and Samali, B. (1992), “Control of wind-induced tall building response by tuned mass dampers”, *J. Wind. Eng. Ind. Aerod.*, **40**(1), 1-32. [https://doi.org/10.1016/0167-6105\(92\)90518-F](https://doi.org/10.1016/0167-6105(92)90518-F).
- Yang, G. (2000), “Bohai sea ice conditions”, *J. Cold Reg. Eng.*, **14**(2), 54-67. [https://doi.org/10.1061/\(ASCE\)0887-381X\(2000\)14:2\(54\)](https://doi.org/10.1061/(ASCE)0887-381X(2000)14:2(54)).
- Yue, Q. and Bi, X. (2000), “Ice-Induced jacket structure vibrations in Bohai Sea”, *J. Cold Reg. Eng.*, **14**(2), 81-92. [https://doi.org/10.1061/\(ASCE\)0887-381X\(2000\)14:2\(81\)](https://doi.org/10.1061/(ASCE)0887-381X(2000)14:2(81)).
- Yue, Q., Zhang, L., Zhang, W. and Kärnä, T. (2009), “Mitigating ice induced jacket platform vibrations utilizing a TMD system”, *Cold Reg. Sci. Technol.*, **56**(2-3), 84-89. <https://doi.org/10.1016/j.coldregions.2008.11.005>.
- Zhang, B.L., Han, Q.L. and Zhang, X.M. (2017), “Recent advances in vibration control of offshore platforms”, *Nonlinear Dynam.*, **89**(2), 755-771.

HJ